LOW-COST EXTENDED-GATE FIELD EFFECT TRANSISTOR SENSING SYSTEM BASED ON A CHANNEL STRUCTURED REFERENCE ELECTRODE

Xinran Wang, Yang Tian, Yuncong Chen, Yueyi Jiao, Md. Azahar Ali, Le Wei, and Liang Dong
Iowa State University, Ames, IA, USA

ABSTRACT

This paper reports a low-cost extended-gate field effect transistor based nitrate sensor using a microfluidic channel based Reference Electrode (µcRE). The µcRE is integrated with a MOSFET to increase potential stability for long-term measurement. The sensor also includes a readout circuit to save or remotely transmit data to a smartphone. The µcRE exhibits a 0.5 mV/hour drift rate and the sensor offers a 0.997 R-Squared value to the linear fitting for potentiometric measurement of nitrate in water.

KEYWORDS

Extended-gate FET, microchannel, reference electrode.

INTRODUCTION

The extended-gate field effect transistor (EGFET)-based ion sensor consists of two parts, i.e., an ion-sensitive membrane and a MOSFET [1]. The difference between the EGFET-based ion sensor and ion-selective field effect transistor (ISFET) is the location of sensitive membrane. For EGFET-based sensors, the MOSFET is often designed as part of a readout circuit and only the sensitive membrane contacts test solutions. The EGFET configuration can not only offer a reduced fabrication cost but also eliminate the influence of temperature, light, and erosion by the test solutions on the characteristics of MOSFET [2].

While numerous efforts have been made to improve the sensitivity and selectivity of ion-selective membrane materials for working electrodes (WE) of ion sensors [3-5], reference electrodes (REs) have not been paid attention with the same intensity in spite of its critical importance to maintain potential stability. For silver/silver chloride (Ag/AgCl)-based REs, the reaction at the electrode surface is $\mathrm{AgCl(s) + e^- \rightleftarrows Ag(s) + Cl^-}$. According to Nernst equation, the cell electrochemical potential E is given by

$$E = E^0 - 0.02958\times \log([Cl^-]) \qquad (1)$$

where E^0 is the standard reduction potential that applies when chloride ion concentration ($[Cl^-]$) is equal to 1 M [6]. From Eq. (1), it is clear that in order to maintain the potential E, the $[Cl^-]$ has to be constant. Commercial glass Ag/AgCl REs use a saturated KCl solution as the inner filling electrolyte solution to react with the reference internal element, producing a constant reference potential. The porous plug at the base of the electrode functions as a salt bridge, allowing ions to diffuse between the inner solution inside and outside the electrode with minimal physical mixing. This kind of REs can provide a relatively stable reference potential but suffers from high cost and difficulty in integration and miniaturization. On the other hand, solid-state REs use solid contacts as ion-to-electron transducing layers but do not require any inner filling solutions [7-8]. Many solid-state REs use polyvinyl butyral or polyvinylchloride as a polymer matrix on the top of Ag/AgCl to hold a high concentration of Cl^-. However, the potential drift of these REs is still high due to the inevitable leaching of Cl^- to surrounding test solutions [9, 10]. In spite of the efforts made to optimize the materials for REs, some approaches relating to structural development of REs have also been conducted to minimize the change of chloride ion concentration at the electrode surface, including using a KCl[Ag/AgCl]KCl sandwich structured RE [11], and a microfluidic RE with a 10-100 µm diameter hole [12].

In this work, a low-cost EGFET ion sensor is reported. The sensor integrates a novel microfluidic channel based RE (µCRE) and a MOSFET to improve potential stability for long-term measurement, and meanwhile to reduce the footprint size. The sensor can be applied to continuously monitor changes of ion concentration in environments.

STRUCTURE

The presented EGFET nutrient sensor is composed of a 3D-printed serpentine microfluidic channel with an embedded Ag/AgCl electrode, a mini glass frit with a mean pore size of 7 ± 3 nm, a sample cell, a working electrode (WE), and a printed circuit board (PCB) with readout electronic circuits (Fig. 1). The microfluidic channel is filled with an inner filling electrolyte solution of 3.4 M KCl. A mini glass frit is inserted into an 800 µm-diameter hole through the thin wall separating the microfluidic channel from the sample cell. The Ag/AgCl electrode is placed at the end of the channel filled with the KCl solution, which theoretically offers a stable reference potential without any manual interference, while remaining a small footprint size, as opposed to bulky glass tube based commercial reference electrodes. Essentially, due to osmosis, chloride ions in the liquid electrolyte is still leaching from the channel through the mini frit into the sample cell. However, the chloride in the solid Ag/AgCl won't be affected unless the chloride concentration in the electrolyte solution near to the frit drops to a low level that triggers concentration difference induced leaching. The long thin channel thus will help to increase potential stability over time.

To form a nitrate sensor as a demonstration, we also coat the other Ag/AgCl electrode in the test cell with a nitrate-sensitive membrane. The WE inside the sample cell directly contacts with test solutions. A potential difference between the WE and RE is converted to a current change using the MOSFET, processed by a home-made datalogger, and then transmitted to a smartphone through Bluetooth.

MATERIALS AND MANUFACTURING

Methyltriphenylphosphonium bromide, polyvinyl chloride, nitrocellulose, 2-nitrophenyl octyl ether, tetrahydrofuran, and tridodecylmethylammonium nitrate were purchased from Sigma Aldrich. Ag/AgCl ink (comprised finely dispersed chloridized silver flake) was purchased from Fisher Scientific. Deionized water with

978-1-5386-8104-6/19/$31.00 ©2019 IEEE

resistivity was obtained from a purification system from Millipore and utilized for all experiments. KNO_3 and KCl powders were obtained from Fisher Scientific. Glass frit (CoralPor™1000) was purchased from KOSLOW Scientific. All electronic parts and epoxy were purchased from Digi-key.

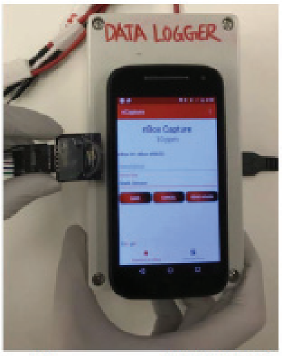

Figure 1: Photo of the proposed EGFET-based nutrient sensor system.

The schematic of 3D-printed case (22 mm × 22 mm × 5 mm) and PCB (22 mm × 30 mm) are shown in Fig. 2. Here, Ag/AgCl paste was firstly screen-printed on the top of the rectangle-shaped RE (10 mm × 2 mm) and round-shaped WE (3 mm diameter), and then was cured at 110 °C for 30 min. The thickness of Ag/AgCl paste (290 µm thickness [13]) was controlled by the thickness of stencil. The 3D-printed case, containing a microfluidic channel [14], was assembled with the PCB using epoxy. The mini glass frit was inserted into the hole to separate the inner filling electrolyte and test solution. The inner filling solution (3.4 M KCl) was filled into the microfluidic channel based container via an inlet. A small outlet was also required for air to flow out of the container. Both the inlet and outlet were sealed by epoxy at last. Here the microfluidic channel with 900 µm width and 20 mm length was designed and placed inside the inner electrolyte container to increase the distance between the Ag/AgCl electrode and the samples to reduce changes of chloride ion concentration around the RE, but still, have the ionic conductivity. By this way, stable reference potential and small device size were achieved. The device is shown in Fig. 2b, where the WE and RE were fabricated on the same side of PCB, while the other side contains all the required electronic devices.

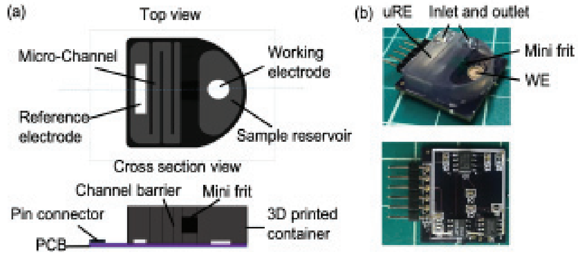

Figure 2: Schematic of the EGFET-based nitrate sensor consisting of a 3D printed case case (a) and a PCB (b). The sensor case contains a sample reservoir, a channel-based container and a hole for a glass frit.

In the nitrate-sensitive membrane, cocktail contains methyltriphenylphosphonium bromide (0.25 wt. %), nitrocellulose (moistened with 2-propanol; 1.93 wt. %), 2-nitrophenyl octyl ether (16.25 wt. %), polyvinyl chloride (5.75 wt. %), tetrahydrofuran (74.3 wt. %), and tridodecylmethylammonium nitrate (1.50 wt. %) [15]. This membrane used an ionophore-doped PVC and was drop-cast on the top of Ag/AgCl paste for the WE. Before use, the WE was pre-conditioned in a 2000 ppm NO_3^--N solution for 12 hr. This step iwass shown crucial to minimize the response of WE to other non-targeted ions such as Cl^- and NH_4^+ [16].

ELECTRONIC CIRCUITRY

The device circuit on the PCB contains two main components, including a MOSFET (ALD110900SAL) and an operational amplifier (LT1462CS8). Here, a potential difference between the working and reference electrodes was generated due to the concentration difference between the sample and inner filling electrolyte solutions. This potential was converted to a current change through an external MOSFET circuit, and then was read and recorded by a home-made datalogger.

The datalogger circuit consists of four modules, including a power module, a readout circuit module, a microcontroller module, and a data transmission module. Its flow chart is shown in Fig. 3b, where the orange, blue, and black arrows represent power transmission, data transmission, and general connections, respectively. The power module provides power for the whole sensor system. The readout circuit captures the electrical voltage potential coming from the sensor electrodes, and then transmits the signal to the microcontroller for data processing. The processed data can be either stored into a micro SD card or be wirelessly transmitted by the Bluetooth module [16].

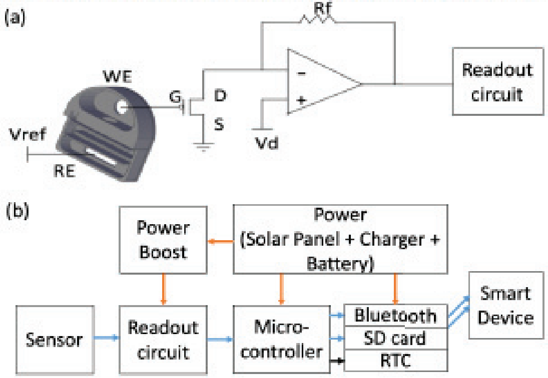

Figure 3: (a) Schematic of the circuit diagram for the EGFET. (b) Flow chart of the electrical system used for data reading and transmission.

RESULTS AND DISCUSSION

RE long-term stability simulation

A finite element analysis method was used to simulate variations of chloride ion concentration for non-channel (nc) and microfluidic channel (µc) structured electrolyte containers. The initial Cl^- concentration was set to 3.4 M, and temperature was set to 24 °C. The simulation results in Fig. 4 shows that for the nc-based RE container, the Cl^-

concentration near the RE started decreasing from the starting point, and after 15 days the Cl^- was run off, while for the µc-based RE container, the Cl^- concentration could remain constant for 2.5 days and then depleted to almost zero after 30 days. Therefore, the longer distance between the RE and test solution, the longer constant time the Cl^- concentration near the RE.

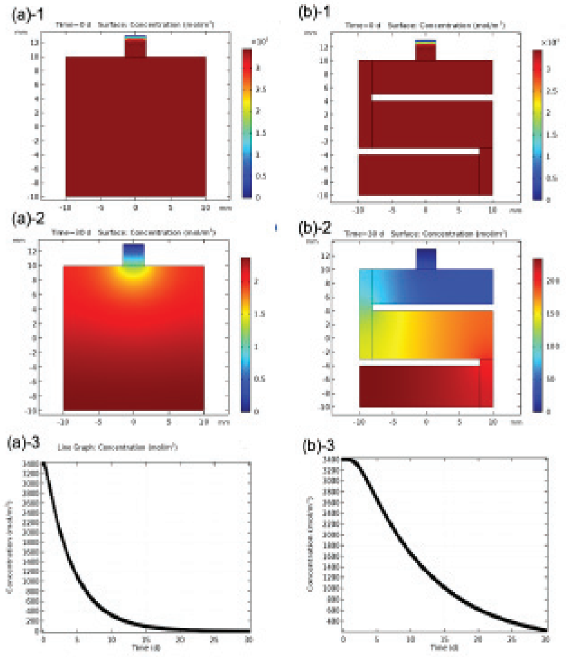

Figure 4: Simulation results of the Cl^- concentration inside the nc (a) and µc structured (b) RE containers. (a)-1 and (b)-1 are the initial concentration status (day 0); (a)-2 and (b)-2 are the 30th-day results, and (a)-3 and (b)-3 are the Cl^- concentration change at the RE point for 30 days.

Chloride susceptibility and long-term stability

To conduct experiments for studying chloride ion susceptibility and long-term stability, the potentials of the nc- and µc-based REs were measured individually against a commercial calomel double junction reference electrode (HANNA Instruments; Model HI5414) where 3.5M KCl served as the inner filling electrolyte. The measurement result was recorded over time. All the measurements were conducted at 24 °C.

For Cl^- susceptibility testing, the experiments were performed in a series of KCl solutions containing 0.01 M, 0.1 M, 0.5 M, and 1.0 M concentration of Cl^-. The experiment time was 5 min for each test solution. From the results shown in Fig. 5a, the potential of the µcRE, from 0.01M to 1M KCl, drifted 4 mV, while for the ncRE, the potential drifted 12 mV. Thus, the µcRE has shown a less susceptibility to Cl^- concentration of the sample solutions, compared to the nc-based RE. Also, Fig. 5a shows that within each 5 min period, the µcRE exhibited a better short-term stability (0.8 mV variation) compared with the nc-based RE (3 mV variation).

The long-term potential stability test was carried out in a beaker containing 0.01M KCl solution and capped to minimize the solution evaporation. For both the REs, the hydration time is about 20 hours, which is defined as the time required for the electrode to reach a stable potential when the electrode placed in a solution. As shown in Fig. 5b, for the first 2 days, the potential of the µcRE remained stabilized, and then it started drifting with a 0.5 mV/hr drift rate, while for the nc-based RE, it started drifting with a 0.8 mV/hr drift rate from the starting point with obvious voltage variations. Therefore, compared with the nc-based RE, the µcRE has a better long-term stability as agreed with the simulation result. Additionally, to further improve the long-term stability, the inner filling (liquid state 3.4 M KCl solution) could be replaced by a filling gel such as agar or gelation serving as a matrix to hold KCl. But, the challenge is that this kind of material is easy to dry in air and also needs high temperature to prepare. Therefore, here a KCl solution was chosen as the inner filling electrolyte.

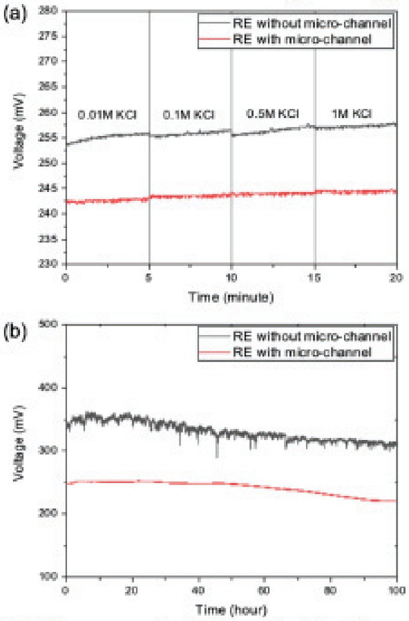

Figure 5: Reference potential against the base potential provided by a commercial calomel double junction RE a function of time in (a) different KCl solutions; (b) 0.01 M KCl for four days. 100 mV offset voltage was added to each potential value at the nc-based RE to help better visualize the actual voltage variation with respect to time.

Nitrogen detection

The nitrate-sensitive membrane was coated on the top of the WE surface to realize the EGFET-based nitrate sensor. The calibration result was plotted in Fig. 6a. The curves represent the potential as a function of nitrate concentration from 0 ppm to 2000 ppm in logrithmic scale. The red curve represents the measured data, and the black curve indicates the linear fitting. The fitting result shows that the slope of the calibration plots of this EGFET sensor is -202.16±5.55 mV/decade with R-Squared vualue of 0.997. Fig. 6b shows the repeatability testing results with maximum 20 mV standard deviation.

CONCLUSIONS

We developed an EGFET-based nitrate sensor with a microfluidic channel based RE. The performance of this RE was characterized in terms of chloride susceptibility and long-term stability. Low chloride responsivity and high long-term potential stability were observed for this sensor.

Due to easy fabrication, small footprint size, high stability, and low cost, this sensor system will be suitable for long-term field sensing applications such as continuous monitoring of nutrient concentration changes in water and soil [18, 19].

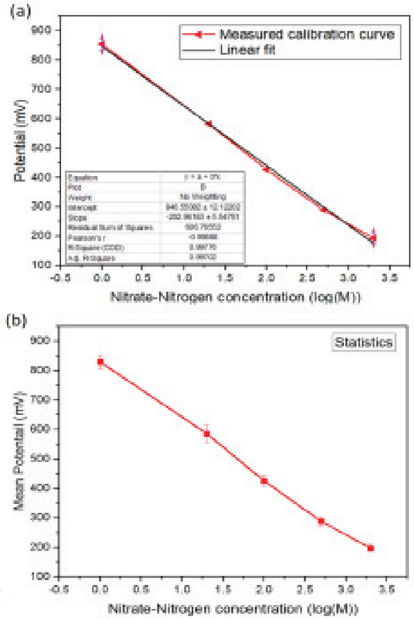

Figure 6: (a) Output voltage of the sensor versus nitrate concentration. (b) Repeatability. The average voltage in every solution was calculated based on 3 rounds of testing.

ACKNOWLEDGEMENTS

The information, data, or work presented herein was funded in part by the Advanced Research Projects Agency-Energy (ARPA-E), U.S. Department of Energy, under Award Number DE-AR0000824. The views and opinions of authors expressed herein do not necessarily state or reflect those of the United States Government or any agency thereof. This project was also partially supported by the United State Department of Agriculture (USDA) under the grant number 2017-67013-26463, and National Science Foundation under the grant number IOS-1650182. The authors also thank Patrick Schnable and Michael Castellano at ISU, and James Schnable at University of Nebraska-Lincoln for discussions.

REFERENCES

[1] P. Salvatore, et al. "EGFET-Based Sensors for Bioanalytical Applications: A Review." Sensors 18.11 (2018): 4042.

[2] Q. Li, et al. "Stable thin-film reference electrode on plastic substrate for all-solid-state ion-sensitive field-effect transistor sensing system." IEEE Electron Device Letters 38.10 (2017): 1469-1472

[3] C.P. Chen, et al. "Ultrasensitive in situ label-free DNA detection using a GaN nanowire-based extended-gate field-effect-transistor sensor." Analytical chemistry 83.6 (2011): 1938-1943.

[4] E.M. Guerra, et al. "Extended gate field effect transistor using V2O5 xerogel sensing membrane by sol–gel method." Solid State Sciences 11.2 (2009): 456-460.

[5] T. Sakata, et al. "Potential behavior of biochemically modified gold electrode for extended-gate field-effect transistor." Japanese Journal of Applied Physics 44.4S (2005): 2860.

[6] D.C. Harris. Exploring chemical analysis. Macmillan, 2012.

[7] I.Y. Huang, et al. "Fabrication and characterization of a new planar solid-state reference electrode for ISFET sensors." Thin Solid Films 406.1-2 (2002): 255-261.

[8] Y.G. Vlasov. "New solid-state ion-selective electrodes—Sensors for chemical analysis of solutions. "Fresenius' Zeitschrift für analytische Chemie 335.1 (1989): 92-99.

[9] T. Kim, et al. "A solid-state thin-film Ag/AgCl reference electrode coated with graphene oxide and its use in a pH sensor." Sensors 15.3 (2015): 6469-6482.

[10] M. Shinwari, et al. "Microfabricated reference electrodes and their biosensing applications." Sensors 10.3 (2010): 1679-1715.

[11] Ł. Tymecki, et al. "Screen-printed reference electrodes for potentiometric measurements." Analytica Chimica Acta 526.1 (2004): 3-11.

[12] M.A.G. Zevenbergen, et al. "Solid state pH and chloride sensor with microfluidic reference electrode." 2016 IEEE International Electron Devices Meeting (IEDM). IEEE, 2016.

[13] A. Simonis, et al. "Miniaturised reference electrodes for field-effect sensors compatible to silicon chip technology." Electrochimica acta 51.5 (2005): 930-937.

[14] L. Dong, et al. Selective formation and removal of liquid microlenses at predetermined locations within microfluidics through pneumatic control. Journal of Microelectromechanical Systems, 17.2 (2008): 381-392.

[15] J. Sutter, et al. "Solid-contact polymeric membrane electrodes with detection limits in the subnanomolar range." Analytica Chimica Acta 523.1 (2004): 53-59.

[16] T. Guinovart, et al. "A reference electrode based on polyvinyl butyral (PVB) polymer for decentralized chemical measurements." Analytica chimica acta 821 (2014): 72-80.

[17] S.S. Sridharamurthy, et al. "A microfluidic chemical/biological sensing system based on membrane dissolution and optical absorption." Measurement Science and Technology 18.1 (2006): 201.

[18] M.A. Ali, et al. "Microfluidic impedimetric sensor for soil nitrate detection using graphene oxide and conductive nanofibers enabled sensing interface." Sensors and Actuators B: Chemical, 239 (2017): 1289-1299.

[19] M.A. Ali, et al. "In situ integration of graphene foam–titanium nitride based bio-scaffolds and microfluidic structures for soil nutrient sensors." Lab on a Chip, 17.2 (2018): 274-285.

CONTACT

*Liang Dong, tel: +1-555-294-0388; ldong@iastate.edu